Reaktor

p-ISSN 0852 – 0798
e-ISSN 2407 – 5973

Website: http://ejournal.undip.ac.id/index.php/reaktor/

Reaktor, Vol. 21 No. 4, December Year 2021, pp. 160-169

Dynamic and Steady Model Development of Two-Chamber Batch Microbial Fuel Cell (MFC)

Ardiyan Harimawan[*)], Hary Devianto, Gilbert, and Jeanny Wijaya

[1)]Department of Chemical Engineering, Faculty of Industrial Technology, Institut Teknologi Bandung
Jl. Ganesha 10, Bandung, Telp.Fax. (022) 2500989/(022) 2501438

[*)]Corresponding author: ardiyan@che.itb.ac.id

(Received: October 18, 2021; Accepted: February 14, 2022)

Abstract

As an alternative source of renewable energy that has piqued researchers' interest, Microbial Fuel Cell's (MFC) limitation of low power density requires further development. Various factors affect the performance, but performing all will be costly and time-consuming. Through a combination of dynamic and steady-state mathematical models modified from past research, the effect of microbe types towards dynamic biofilm formation and steady-state OCV can be observed, followed by steady-state simulation to determine maximum power density and its' corresponding voltage. Similarity with previous research has been observed, with a maximum OCV of 838.93 mV achieved by heterotrophic biomass in 75-100 hours with biofilm thickness of 2.087 x 10^{-4} m, while generating maximum power density of 2050.12 mW//m^2 and voltage of 408.16 mV. The lowest OCV value of 838.76 mV was observed in C. sporogenes in 450-475 hours with a biofilm thickness of 2.079 x 10^{-4} m, while the lowest value of maximum power density was observed in anaerobic microbial communities at 8.48 mW/m^2 with the voltage of 90.43 mV. Furthermore, it has been observed that variations with higher μ_{max} and lower K_s result in higher steady-state OCV in the shortest amount of time, while increasing power density and its' corresponding voltage.

Keywords: *biofilm; cell voltage; mathematical model; OCV; power density*

How to Cite This Article: Harimawan, A., Devianto, H., Gilbert, and Wijaya, J., (2021), Dynamic and Steady Model Development of Two-Chamber Batch Microbial Fuel Cell (MFC), Reaktor, 21(4), 161-170, https://doi.org/10.14710/reaktor.21.4.161-170

INTRODUCTION

The urgency of renewable energy is increasing in the world. Up until now, energy demand heavily relies on fossil fuels. The high generation of carbon emissions accelerating climate change and the declining supply of fossil fuels urge the development of alternative renewable energy sources. Microbial fuel cell (MFC) is one of the renewable energy technologies with promising potential, utilizing microbes as the catalyst to generate energy while offering various advantages that attract researchers, for instance, operated at room temperature, utilizing waste as substrate for the microbes, and does not produce waste nor carbon emission.

In general, MFC has the same working principles as a fuel cell (FC). MFC has two chambers, anode chamber and cathode chamber which are separated by a proton exchange membrane (PEM). The main difference between MFC and FC is at the anode chamber, MFC uses microbial reaction while

FC uses inorganic substance reaction to produce electrons. In the anode chamber, microbes oxidize substrate to produce electrons and protons, electrons are transferred through an external circuit, while protons are transferred to the cathode chamber. In the cathode chamber, oxygen acts as final electron acceptors as the result of high redox potential and low operating cost (Chou *et al.*, 2013; Fitzgerald *et al.*, 2013).

As MFC utilizes microbes to produce electrons, the type of culture microbes used will affect the amount of electron generation. In most cases, mixed culture microbes are chosen for MFC as they produce a higher power density compared to pure culture microbes (Rabaey *et al.*, 2003). In mixed culture microbes, there is more variety of exoelectrogens, which could also contribute to electric generation (Cao *et al.*, 2019). However, the research of exoelectrogens is mostly done using pure culture microbes (Fauzi, 2018). The operations using pure culture are strict, for example being aseptic. This condition is hard to achieve if the MFC is operated using waste.

Aside from types of microbial culture, many factors affect the performance of MFC. Investigating all individually will be costly and time-consuming, as such an MFC system could be optimized using the availability of suitable mathematical models. The mathematical models offer equations that explain the phenomenon of the MFC system, give a deeper understanding of the MFC operation, help identify and correct the bottlenecks of the main processes (Ortiz-Martinez *et al.*, 2015). This work aims to determine the kinetic effect of microbial culture towards simulation results in both dynamic and steady-state condition.

METHODOLOGY

In this work, the mathematical model consists of two main models, the dynamic model and the steady model. The dynamic model is made using Matlab R2018a software while the steady model is made using Microsoft Excel. The dynamic model is built using Esfandyari *et al.* (2017) with modifications.

Data Collection

Data is collected from experimental data performed by Suryaga (2017) and literature studies to be used as input for the developed model. Various assumptions based on literature are used to limit the scope of research and to provide parameters not obtained through Suryaga (2017) and literature study.

Data Simulation Flowchart

Research steps for dynamic simulation are shown as a flowchart in Figure 1, while the flowchart for steady-state simulation is shown as a flowchart in Figure 2.

The mathematical model simulation consists of dynamic and steady conditions. To achieve the highest voltage and power density of the MFC, the operation will be conducted without any electric circuit or resistor to achieve steady open circuit voltage (OCV). The dynamic model is performed to identify the time required to achieve steady OCV and the effect of biofilm on the OCV. The mathematical model is adapted from the batch mode model developed by Esfandyari *et al.* (2017). The general kinetic equation used to express the electron generation for the dynamic model is expressed as the Nernst-Monod equation in Equation 1.

$$r_s = \mu\left(\frac{1}{1+exp\left(-\frac{F}{RT}\eta_{act}\right)}\right)\phi_a \quad (1)$$

where: r_s is the substrate consumption rate; μ is the specific growth rate, F is Faraday constant, T is the operating temperature, η_{act} is the activation overpotential and ϕ_a is the volume fraction of the active biomass.

In the biofilm, it is assumed that the substrate is diffused into the biofilm and then oxidized by the active biomass. The products are then diffused back into the bulk liquid. As such, five mass balance equations govern the rate of change for each species, namely active biomass, inactive biomass, substrate, dissolved CO_2, and H^+ (Kazemi *et al.*, 2015). The equations expressing the rate of change for biofilm species are shown from Equation 2 through to Equation 6. Assuming that $\phi_a + \phi_i = 1$, biofilm thickness is expressed by Equation 7.

$$\frac{d}{dt}(\phi_a) = Y_{ac}r_s - b_{ina}\phi_a + \frac{\phi_a}{L}\delta - \frac{\phi_a}{L}\frac{d}{dt}(L) \quad (2)$$

$$\frac{d}{dt}(\phi_i) = b_{ina}\phi_a + \frac{\phi_i}{L}\delta - \frac{\phi_i}{L}\frac{d}{dt}(L) \quad (3)$$

$$\frac{d}{dt}(C_s) = \frac{D_s}{L_l L}(C_{sb} - C_s) - \rho r_s - \frac{Cs}{L}\frac{d}{dt}(L) \quad (4)$$

$$\frac{d}{dt}(C_{CO_2}) = \frac{D_{CO_2}}{L_l L}\left(C_{CO_{2_b}} - C_{CO_2}\right) + \rho r_s - \frac{C_{CO_2}}{L}\frac{d}{dt}(L) \quad (5)$$

$$\frac{d}{dt}(C_H) = \frac{D_H}{L_l L}\left(C_{H_b} - C_H\right) + 4\rho r_s - \frac{C_H}{L}\frac{d}{dt}(L) \quad (6)$$

$$\frac{d}{dt}(L) = Y_{ac}r_s L + \delta \quad (7)$$

where: Y_{ac} is the bacterial yield; b_{ina} is the inactivation coefficient; L is the biofilm thickness; δ is the detachment rate calculated as $\delta = -b_{det}L$; b_{det} is the detachment coefficient; ϕ_i is the volume fraction of inactive biomass; L_l is the laminar diffusion sublayer thickness; $D_{s/CO2/H}$ is the substrate/CO_2/H^+ diffusivity; $C_{s/CO2/H}$ is the substrate/CO_2/H^+ concentration; $C_{sb/CO2b/Hb}$ is the bulk substrate/CO_2/H^+ concentration and ρ is the biomass density.

In the anolyte, it is assumed that the pH of the anolyte is constant, resulting in only substrate and CO_2

as the only species with changing bulk concentration. Considering the thickness of biofilm changing over time, the volume changes of the bulk liquid are expressed as Equation 8.

$$\frac{d}{dt}(V_L) = -A_m \frac{d}{dt}(L) \quad (8)$$

where: V_L is the volume of bulk liquid and A_m is the area of biofilm interface.

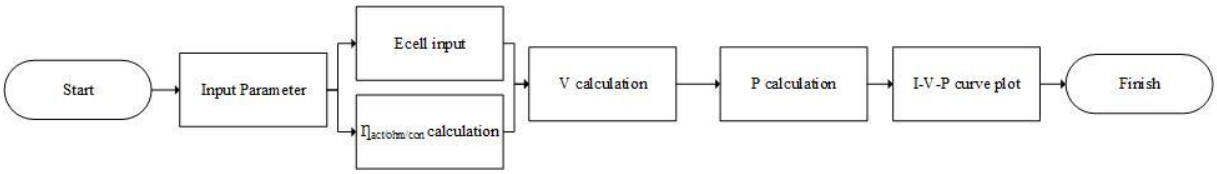

Figure 1. Flowchart of Dynamic simulation

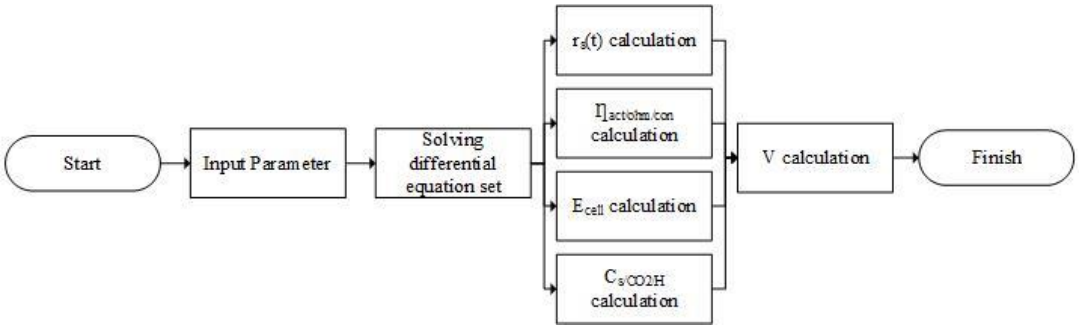

Figure 2. Flowchart of steady-state simulation

The obtained bulk liquid volume is then used to calculate the rate of change of bulk concentration for anolyte species. The mass balances involved in the anodic chamber are expressed by Equation 9 and Equation 10.

$$\frac{d}{dt}\left(C_{s_b}\right) = \frac{1}{V_L}\left(-\frac{A_m D_s}{L_l}\left(C_{s_b} - C_s\right)\right) \quad (9)$$

$$\frac{d}{dt}\left(C_{CO_2{}_b}\right) = \frac{1}{V_L}\left(-\frac{A_m D_{CO_2}}{L_l}\left(C_{CO_2{}_b} - C_{CO_2}\right)\right) \quad (10)$$

In the cathodic chamber, two terminal electron acceptors are present: oxygen and $KMnO_4$. Due to the higher reduction potential of $KMnO_4$ compared to oxygen, it is assumed that only $KMnO_4$ will be reduced in the cathodic chamber, resulting in constant oxygen concentration.

The real voltage of MFC is less than the theoretical one, due to overpotentials which have been described by Esfandyari *et al.* (2017) to be mainly contributed by ohmic, concentration, and activation overpotentials. Measuring OCV where the current does not flow in the model results in zero value in overpotentials. The general electrochemical equations used for the dynamic model are expressed by Equation 11.

$$E_{cell} = E_{thermo} - \eta_{act} - \eta_{con} - \eta_{ohm} \quad (11)$$

where: E_{cell} is the voltage produced from MFC cell; E_{thermo} is the theoretical voltage of the potential difference between anode and cathode; η_{act} is activation overpotential; η_{con} is concentration overpotential; η_{ohm} is ohmic overpotential.

Based on experimental conditions used by Suryaga (2017), acetate and $KMnO_4$ are used as substrate and electron acceptor respectively, with the following standard reduction potentials (Logan, 2008). Based on the electrochemical reactions, the value of potential in the cathode and anode are expressed by Equation 12 and Equation 13.

$$E_{cathode} = E^0_{cathode} - \frac{RT}{3F}\left(\frac{[MnO_2]}{[H^+]^4[MnO_4^-]}\right) \quad (12)$$

$$E_{anode} = E^0_{anode} - \frac{RT}{8F}\left(\frac{[CO_2][HCO_3^-][H^+]^8}{[CH_3COO^-]}\right) \quad (13)$$

The steady model is performed to identify the voltage produced based on the highest current density and the highest power density produced by the MFC system. The mathematical model used from the combination of continuous steady state mathematical model by Zeng *et al.* (2010), the adaptation of continuous mode to batch mode by Oliveira *et al.* (2018), and the modification of the combination model to adjust for Suryaga (2017) experiment by Kautsar and Sualing (2021). The general equations for the steady condition model are expressed by Equation 14.

$$r = \frac{I}{n \times F} \quad (14)$$

where: r is the reaction rate per area; I is the current density; n is the number of electrons involved in the reaction.

The voltage cell value is calculated using Equation 11 with considering the overpotential value. The activation overpotential is the potential loss

caused by the complex reaction on the surface of the electrode (Scott, 2015). The equation to calculate activation overpotential is shown in Equation 15.

$$r_a = \mu_{max} \frac{C_s}{C_s + K_s} C_x \, exp\left(\frac{\alpha_a F}{RT} \eta_a\right) \quad (15)$$

where: r_a is the reaction rate per anode area; μ_{max} is the maximum specific growth rate; K_s is half-velocity constant; C_x is the concentration of biomass; α_a is coefficient of charge transfer in anodic reaction; R is the gas constant; T is temperature.

The value of C_s is calculated by assuming anode chamber as a continuous stirred-tank reactor (CSTR) shown in Equation 16. Equation 17 is the modified Zeng *et al.* (2010) equation using Oliveira *et al.* (2018) equation by Kautsar and Sualing (2021) with the assumption that natural convection through a vertical plane (Cengel, 2002) will occur and is correlated to Sherwood number (Sh). Sherwood number is calculated using Rayleigh number (Ra) and Schmidt number (Sc) in Equation 18, which require the calculation of Grashoff number (Gr) shown through Equation 19 through to Equation 21.

$$\frac{V_a}{A_m} \frac{dC_s}{dt} = \frac{Q_a}{A_m} (C_s^0 - C_s) - r_a \quad (16)$$

$$\frac{V_a}{A_m} \frac{dC_s}{dt} = h_{mass}^s (C_s^0 - C_s) - r_a \quad (17)$$

$$Sh = \frac{h_{mass}^s L}{D_s} \left[0.825 + \frac{0.387 \, Ra^{\frac{1}{6}}}{\left(1 + \left(\frac{0.492}{Sc}\right)^{\frac{9}{16}}\right)^{\frac{8}{27}}} \right]^2 \quad (18)$$

$$Ra = GrSc \quad (19)$$

$$Gr = \frac{g \Delta C L^3}{C v^2} \quad (20)$$

$$Sc = \frac{v}{D} \quad (21)$$

where: V_a is the volume of anode chamber; Q_a is the flow rate of substrate in anode chamber; A_m is the surface area of the membrane; h_{mass}^s is mass transfer coefficient of substrate; C_s^0 is the initial concentration of substrate; L is the electrode length; D is the diffusivity of substrate on anode; g is the gravity acceleration; v is the kinematic viscosity of substrate on anode.

The biomass concentration (C_x) is calculated using the modified Zeng *et al.* (2010) equation using Oliveira *et al.* (2018) equation by Kautsar and Sualing (2021) as shown in Equation 22.

$$\frac{V_a}{A_m} \frac{dC_x}{dt} = r_a \times Y_{\frac{x}{A}} - \frac{V_a \times K_{dec} \times C_x}{A_m} \quad (22)$$

where: $Y_{\frac{x}{A}}$ is the yield of biomass per substrate; K_{dec} is the decay constant of biomass.

The concentration overpotential is the potential loss caused by mass transfer limitations of different species transported to or from the electrode (Oliveira *et al.*, 2018). Oliveira *et al.* (2018) assumed that the concentration overpotential is affected by the cathode overpotential value and is dependent on mass transfer. The concentration overpotential is calculated using Equation 23.

$$r_c = I_{ref} \frac{C_r}{C_{r,ref}} exp\left(\frac{\alpha_c F}{RT} \eta_c\right) \quad (23)$$

where: r_c is the reaction rate per cathode area, I_{ref} is current exchange density of reduced substances at reference condition; $C_{r,ref}$ is the concentration of reduced substances at reference condition; α_c is the coefficient of charge transfer in cathodic reaction.

The concentration of reduced substances (C_r) is calculated using Zeng *et al.* (2010) equation modified using Oliveira *et al.* (2018) equation by Kautsar and Sualing (2021) shown in Equation 24.

$$\frac{V_c}{A_m} \frac{dC_r}{dt} = h_{mass}^r (C_r^0 - C_r) - r_c \quad (24)$$

where: V_c is the volume of cathode chamber; h_{mass}^r is mass transfer coefficient of reduced substance; C_r^0 is the initial concentration of reduced substance.

The ohmic overpotential is the potential loss caused by the resistance of the flow of ions in electrolytes and electrons through an external circuit (Oliveira *et al.*, 2018). Oliveira *et al.* (2018) assumed that the ohmic overpotential is only affected by the membrane. The equation for ohmic overpotential is shown in Equation 25 while the resistance of the cell (R_{cell}) is calculated using Equation 26.

$$\eta_{ohmic} = I_{cell} R_{cell} \quad (25)$$

$$R_{cell} = \frac{\delta^M}{\kappa} \quad (26)$$

where: I_{cell} is the density current; δ^M is the membrane thickness; κ is the conductivity of the membrane.

Model Validation

The result of model validation for the dynamic simulation is as shown in Figure 3. Both simulated data and experimental data obtained from Suryaga (2017) are shown in superposition to compare the results.

Based on Figure 3, similarity in trend was observed when comparing simulation results and

experimental results by Suryaga (2017). According to Ullah (2019), two stages can be observed during OCV measurement. The first is the stage of rapid increase, indicating a rapid formation of microbial culture on the surface of the anode, followed by a maximum OCV value in the second stage due to saturated microbial growth. The difference in time taken to reach steady-state OCV was observed, due to the limitation in the model which depends heavily on kinetic parameters and is limited to pure culture, thus no prediction on the phenomenon of inter-microbial interaction can be observed.

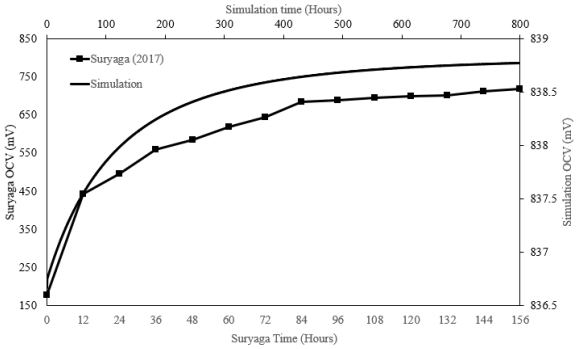

Figure 3. OCV curve of both model and Suryaga (2017) experiment

Under the assumption that acetate was used as the sole substrate, and $KMnO_4$ as the sole oxygen acceptor, theoretical OCV was predicted to reach up to 1830 mV. Compared to the simulation results with the highest value of OCV at 839 mV, a large gap was observed. This is caused by the diffusion phenomenon in the membrane. According to Ahualli (2014), mixing will result in lower potential between both chambers due to foreign ionic species being introduced to the chamber. Although it must be noted that the performance of MFC does not solely depend on OCV value. Further measurement of maximum power density through steady-state simulation can be done to determine the performance of the MFC.

The result of model validation for the steady condition is as shown in Figure 4. Both data experiments from Suryaga (2017) and model plot were being superposition to compare the results. Based on Figure 4, the power density model has not reached maximum power density while the power density experiment has reached the maximum power density of 25.22 mW/m^2 at 52.79 mA/m^2. The power density experiment has a higher value than the power density model at a lower current density. This is caused by the mixed culture (POME and cow manure) used in Suryaga (2017) has higher μ_{max}, but at the same time, the MFC system contains methanogens that compete with exoelectrogens for substrates so the power density drops after reaching 52.79 mA/m^2.

Based on Figure 4, the cell voltage curve drops significantly due to activation overpotential marked by part A. Activation overpotential occurred due to the complex reaction on the electrode surface (Scott, 2015). In this simulation, the complex reaction only considered microbial reaction with the assumption that the biochemistry reaction is much slower than the electrochemical reaction (Zeng *et al.*, 2010). The second cell voltage loss is caused by ohmic overpotential marked as part B. Ohmic overpotential is occurred because of mass transfer limitation.

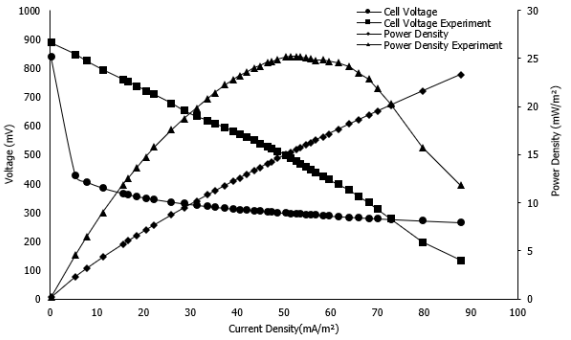

Figure 4. I-V-P curve of both model and Suryaga (2017) experiment

The cell voltage experiment curve drops linearly, it can be concluded that the MFC system experiment is only affected by ohmic concentration. The difference in ohmic overpotential between experiment and model could be caused by different assumptions used. In this model, the ohmic overpotential is affected by membrane resistance only. Concentration overpotential happens after the current density exceeds a specific current density (I_{limit}). I_{limit} is calculated using Equation 27 (Scott, 2015).

$$I_{limit} = nFC\frac{D}{\delta^M} \qquad (27)$$

In this simulation, the value of I_{limit} is 9320 mA/m^2. Based on Figure 4, it can be concluded that the MFC system has not reached the I_{limit} value, so the potential loss is still not affected by concentration overpotential.

Assumption and Limitation

The conducted research employs the following assumptions in the development of both models:

- Proposed models are for two chambers MFC operated in batch mode
- POME as the substrate used is assumed to be acetate
- Dynamic modelling only depends on time (zero dimension)
- MFC are divided to bulk liquid in anode chamber and cathode chamber and biofilm attached to the anode
- Electrode resistance and ion-exchange membrane resistance are negligible
- Both anode and cathode chamber are operated at a constant pH of 7 at constant pressure and temperature
- Operation is performed at 25ºC

- Mass transfer on electrode happens through diffusion
- In dynamic simulation, mass transfer through membrane happens through diffusion
- Concentration of species at the electrode surface is equal to the concentration of species in bulk liquid

Experiment Variation

The variation microbial cultures only used maximum specific growth rate (μ_{max}) and half-velocity constant (K_s). Based on Suryaga (2017), the substrate used is POME and the inoculum is cow manure. The POME also contains microbial cultures which could act as biocatalysts. The kinetic characteristics of the microbial cultures were chosen by approaching POME as wastewater from wastewater treatment plant (WWTP) and cattle manure as cattle manure. The kinetic data used for the mathematical model are shown in Table 2.

MFC is operated under an open circuit to determine the OCV without any external resistance. Time was adjusted between 0 – 800 hours with an interval of 0.5 hours for 6 types of microbes. The obtained curve is shown in Figure 5.

Based on Figure 5, heterotrophic biomass was observed to generate the highest steady-state OCV at 838.93 mV, followed by acidogenesis bacteria and mixed anaerobic microbes. A trend was observed when comparing kinetic parameters from Table 2, where variations with higher μ_{max} will result in higher microbial growth, thus increasing the maximum value of steady-state OCV. This trend was well observed with all variations except *C. cadaveris* and *C. sporogenes*, with μ_{max} far a higher compared to others, but has lower OCV. According to Wang (2015), microbes with higher growth rate will have a faster deactivation rate, thus won't be able to utilize substrate resulting in lower OCV. Lower K_s values will result in better substrate affinity, allowing better efficiency in substrate utilization (Mudler, 2014).

Table 2. Kinetic variable data of microbial cultures

No.	Species	μ_{max} (1/hour)	μ_{max} (1/day)	K_s (g/L)	K_s (mol/m^3)	Substrate	Reference
			Acidogenesis Pure Culture				
1	*Clostridium cadaveris*	0.311	7.464	4.241	70.624	Biological wastewater treatment	Koo *et al.* (2019)
2	*Clostridium sporogenes*	0.360	8.640	5.171	86.112	Biological wastewater treatment	Koo *et al.* (2019)
3	Acidogenesis bacteria	0.168	4.025	0.208	3.469	POME	Lim and Vadivelu (2019)
			Mixed Culture				
4	Mixed anaerobic microbes	0.004	0.086	0.012	0.200	Dairy manure	Lin (1995)
5	Anaerobic microbe communities	0.003	0.070	0.011	0.187	POME	Wong *et al.* (2014)
6	Heterotrophic biomass	0.007	0.167	0.027	0.441	Wastewater treatment plant influent	Krieg *et al.* (2017)

RESULTS AND DISCUSSION

Variation of Microbial Culture on Open Circuit Voltage (OCV)

Variation of microbial culture will result in variation of kinetic parameters μ_{max} and K_s shown in Table 2.

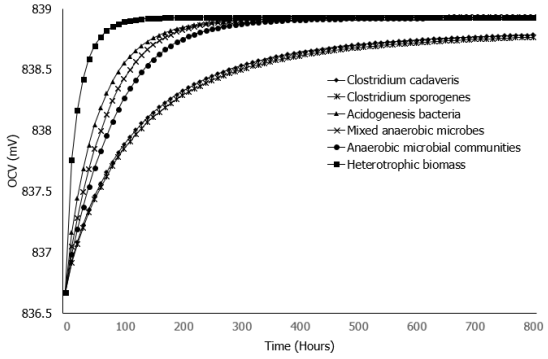

Figure 5. OCV curve of various microbial culture

Compared to μ_{max}, K_s will affect the time consumed to reach steady-state OCV. More efficient substrate utilization will lead to better biofilm formation, and decrease the time required to reach steady-state (Owens, 1987).

Variation of Microbial Culture on Biofilm Thickness

The results for substrate consumption rate and biofilm thickness are shown in Figure 6 and Figure 7. Based on Figure 7, *C. cadaveris* and *C.* sporogenes have the lowest substrate consumption rate, resulting in higher substrate concentration at the end of measurement. higher μ_{max} value will indicate a faster microbial growth rate, but if not coupled with a low K_s value, microbe won't be able to utilize substrate effectively. This indicates a slower consumption rate, even if the microbial growth rate is fast (Sakthiselvan, 2019).

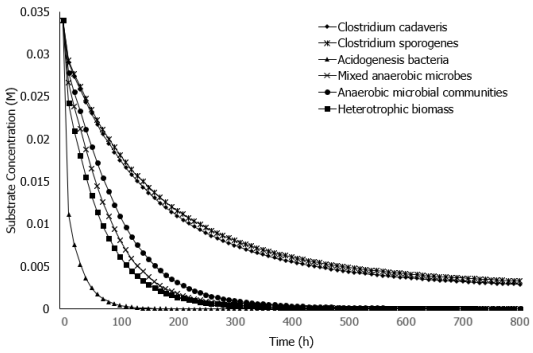

Figure 6. Substrate concentration curve with various microbial culture

As a result, microbes with lower K_s value coupled with high μ_{max} will have the highest substrate consumption rate, as evidence by heterotrophic biomass. According to Wang (2015), the thickness of a biofilm will reach a stable value when all substrate is consumed, in which the microbial growth is stopped.

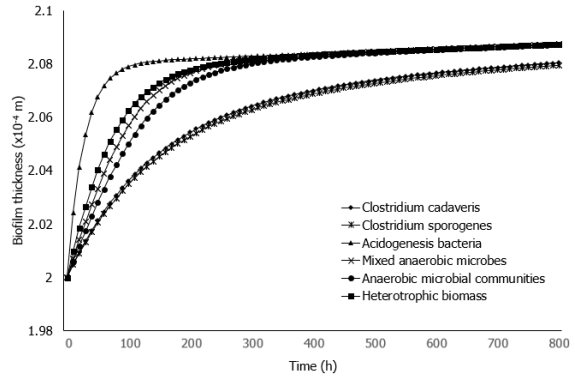

Figure 7. Biofilm thickness curve with various microbial culture

Based on Figure 7, heterotrophic biomass has the highest substrate consumption rate, thus resulting in thicker biofilm and faster biofilm formation compared to other variations. According to Marcus (2007), a thicker biofilm will contribute to a more active fraction of biomass and increase the maximum value of steady-state OCV an MFC can reach. Comparing Figure 7 to Figure 5 shows that the trend agrees well with previously conducted research by Marcus (2007).

Variation of Microbial Culture on I-V Curve

Variation microbial culture on I-V curve is performed by variating kinetic parameters such μ_{max} and K_s shown in Table 2. The initial theoretical voltage cell (E_{thermo}) value is using the steady OCV value from the dynamic model. The initial concentration value of the microbial culture variation (C_s^0) was adjusted to 34 mmol/m^3 as this value affects the value of r_a and η_a as shown in Equation 16.

Based on Figure 8 at 87.83 mA/m^2, heterotrophic biomass produces the highest voltage, followed by *C. sporogenes* and *C. cadaveris*. This trend happens because voltage value is affected by μ_{max} and K_s as shown in Equation 2.18. Based on Table 2, *C. sporogenes* and *C. cadaveris* have the highest value of μ_{max} however their K_s value is also high which means the affinity of the microbial culture towards substrate used is not favorable which leads to reduction of electron production. According to Kautsar and Sualing (2021), the effect on K_s towards cell voltage is not significant compared to μ_{max}. However, if the difference of K_s is much higher such as *C. cadaveris* and heterotrophic biomass value shown in Table 2, it could reduce the voltage cell and it is proved as shown in the simulation.

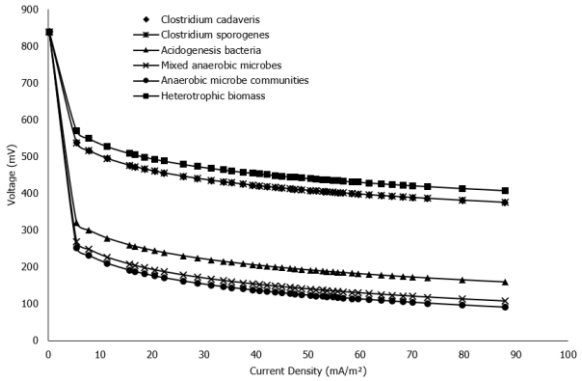

Figure 8. I-V curve obtained from variation of microbial culture

Variation of Microbial Culture on I-P Curve

Variation microbial culture on I-P curve is performed by variating kinetic parameters such μ_{max} and K_s shown in Table 2. The power density value is calculated by multiplying the voltage value and current density value from the steady model. The initial concentration value of C_s^0 is also adjusted the same as in I-V curve calculation.

Based on Figure 8 at 87.83 mA/m^2, heterotrophic biomass produces the highest voltage, followed by *C. sporogenes* and *C. cadaveris*. This order of the power density produced has the same trend with the I-V curve because power density is calculated using voltage value which is affected by μ_{max} and K_s as shown in Equation 16.

In general, heterotrophic biomass gives the best performance with the highest value of steady OCV, voltage, and power density. However, compared to other mixed cultures, heterotrophic biomass has higher μ_{max}. According to Krieg *et al.* (2017), the research is done by performing an aerobic condition in the anode chamber (partially aerobic, under low dissolved oxygen concentration). In this condition, facultative anaerobic bacteria in mixed culture could grow faster as they change the fermentation metabolism to aerobic respiration (Mshandete *et al.*, 2005; O'Keefe and Chynoweth, 2000). However, the value of μ_{max} does not lead to higher electricity production because in the anode chamber the dissolved oxygen tends to form water by utilizing the electron produced by the microbial culture (Ringeisen *et al.*, 2007). Another problem with using POME and

cow manure is it contains non-exoelectrogens bacteria such as methanogens which compete with exoelectrogens such as acetogenic bacteria for the carbon source. Therefore, mixed cultures with higher μ_{max} do not necessarily produce higher cell voltage.

Mixed culture microbes tend to have higher μ_{max} compared to the pure culture in the same operating condition. However, mixed anaerobic microbes and anaerobic microbe communities have a lower value of μ_{max} value than pure cultures *C. cadaveris*, *C. sporogenes*, and acidogenesis bacteria. Other factors affect μ_{max} value, such as the type of substrate and initial substrate concentration. According to Borschers *et al.* (2013), each microbe has its preference on the substrate that could be easily metabolized which leads higher growth rate on the specific substrate.

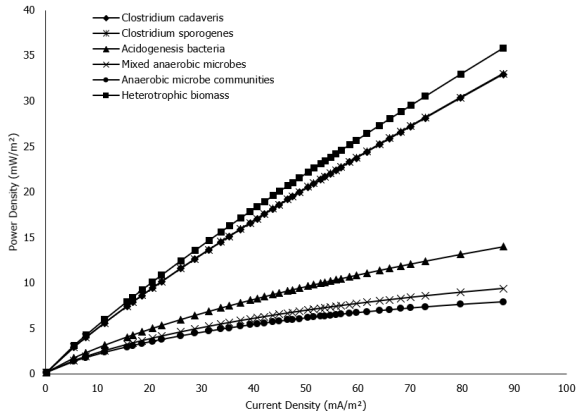

Figure 9. I-P obtained from variation of microbial culture

In Table 2, each experiment has a different initial substrate concentration which also affects the value of μ_{max}. Aside from μ_{max}, K_s value also affects the MFC performance. K_s value is also affected by the type of substrate used (Mulder and Hendriks, 2014) and the type of microbes as they have their preference on the type of carbon source (Carpenter and Guillard, 1971). As there are a lot of variables that can affect the MFC performance, using this mathematical model as an initial trial test can help reduce the time required for the experiment need. In addition to identifying and eliminating experiment candidates that show deviation, this model can help determine which culture will potentially generate the highest OCV, voltage, power density, the concentration of substrate used, biofilm thickness from the MFC system.

STATISTICAL COMPARISON

Comparison between both independent groups of OCV measured through experimentation by Suryaga (2017) and from the model are done in order to determine the difference from a statistical viewpoint through the Analysis of Variance (ANOVA).

Using a value of 0.05 for the significance level of test results in a P-value of 2.83 x 10^{-6}, indicating that both variations are significantly different. The difference is due to the limitation in model which heavily depends on kinetic parameters and is limited to pure culture, while experimentations are done using a mixed culture of which the model was unable to predict the phenomenon of inter-microbial interaction. The effect of synergy between various microbe in mixed culture can be further investigated in another separate research.

Table 3. Analysis of variance (ANOVA) on OCV

Time (h)	OCV (mV)	
	Model	Experiment
0	836.67	179.00
12	836.95	442.00
24	837.12	495.00
36	837.28	559.00
48	837.41	585.00
60	837.53	618.00
72	837.64	644.00
84	837.74	683.00
96	837.82	689.00
108	837.90	695.00
Time (h)	OCV (mV)	
	Model	Experiment
120	837.97	699.00
132	838.03	701.00
144	838.09	712.00
156	838.14	717.00

Variation Source	Average	Variance	Sum of Squares
Model	837.59	0.20	390882.46
Experiment	601.28	22110.99	287445.52
P-value		2.83 x 10^{-6}	
F crit		4.23	

CONCLUSION

As inferred from the simulation, the value of kinetic parameters μ_{max} and K_s influenced the results of both dynamic and steady-state simulations. In the dynamic simulation, a higher value of μ_{max} will increase the maximum value of OCV generated by the MFC due to the higher growth rate and microbial biofilm forming on the surface of the anode contributing towards higher OCV generation. A higher value of μ_{max} will also increase microbial deactivation rate, and thus contributes negatively to the maximum OCV value. Lower K_s value will shorten the amount of time required to reach steady-state OCV, mainly because K_s positively contributes towards the rate of substrate consumption. A higher rate of substrate consumption will lead to depletion of substrate available for the MFC, causing OCV value to reach the steady-state. While in steady-state simulation, the higher value of μ_{max} indicates the faster growth rate of microbial culture that can generate electrons which lead to higher generation of voltage. Lower K_s indicates the high affinity of microbes towards the substrate being used, generating

more electrons compared with a higher value of K_s which also leads to a higher generation of voltage. This simulation model can help reduce experiment time since the microbial related experiment required much longer time compared to a non-biological experiment.

REFERENCES

Ahualli, S., Fernandez, M.M, Iglesia, G., Jimenez, M.L., Liu, F., Wagterveld, M., Delgado, A.V., (2014), Effect of Solution Composition on the Energy Production by Capacitive Mixing in Membrane-Electrode Assembly, *J Phys Chem C Nanometer Interfaces*, 118(29), pp. 15590-15599.

Borschers, S., Freund, S., Rath, A., Streif, S., Reichl, U., Findeisen, R., (2013), Identification of Growth Phases and Influencing Factors in Cultivations with IAGE1.HN Cells Using Set-Based Methods, *PloS ONE, 8(8), pp. 68-124*

Cao, Y., Mu, H., Liu, W., Zhang, R., Guo, J., Xian, M., Liu, H., (2019), Electricigens in the anode of microbial fuel cells: pure cultures versus mixed communities, *Microbial Cell Factories*, 18(1), pp. 18-39

Carpenter, E.J., Guillard, R.R.L., (1971), Intraspecific differences in nitrate half-saturation constants for three species of marine phytoplankton, *Ecology*, 52(1), pp. 183-185

Cengel, Y.A., (2002), *Heat Transfer: A Practical Approach*, 2nd, McGraw-Hill, New York, pp. 466-473

Chou, T.Y., Whiteley, C.G., Lee, D.J., Liao, Q., (2013), Control of dual-chambered microbial fuel cell by anodic potential: Implications with sulfate reducing bacteria, *International Journal of Hydrogen Energy*, 38(35), pp. 15580-15589

Esfandyari, M., Fanaei, M. A., Gheshlaghi, R., Akhavan Mahdavi, M., (2017), Mathematical modeling of two-chamber batch microbial fuel cell with pure culture of Shewanella, *Chemical Engineering Research and Design*, 117(1), pp. 34–42

Fauzi, A., (2018), Optimation of Microbial Fuel Cell (MFC) Performance to Increase Electricity, *Master's Thesis*, Institut Teknologi Bandung, Indonesia.

Fitzgerald, L.A., Petersen, E.R., Leary, D.H., Nadeau, L.J., Soto, C.M., Ray, R.I., Little, B.J., Ringeisen, B.R., Johnson, G.R., Vora, G.J., (2013), Shewanella frigidimarina microbial fuel cells and the influence of divalent cations on current output, *Biosensors and Bioelectronics*, 40(1), pp. 102- 109

Kautsar, R. B., Sualing, J., (2021), Model of Bioelectrochemical Process from Two Chamber MFC with Batch System, *Undergraduate's Thesis*, Institut Teknologi Bandung, Indonesia.

Kazemi, M., Biria, D., Rismani-Yazdi, H., (2015), Modelling Bio-Electrosynthesis in a Reverse MFC to Produce Acetate from CO2 and H2O, *Physical Chemistry Chemical Physics*, 17(19), pp. 125612-12574

Koo, T., Lee, J., Hwang, S., (2019), Development of an interspecies interaction model: An experiment on Clostridium cadaveris and Clostridium sporogenes under anaerobic condition, *Journal of Environmental Management*, 237(1), pp. 247–254

Krieg, T., Enzmann, F., Sell, D., Schrader, J., Holtmann, D., (2017), Simulation of the current generation of a microbial fuel cell in a laboratory wastewater treatment plant, *Applied Energy*, 195(1), pp. 942–949

Lim, J. X., Vadivelu, M. V., (2019) Enhanced volatile fatty acid production in sequencing batch reactor: Microbial population and growth kinetics evaluation, *6th International Conference on Environment (ICENV2018) AIP Conference Proceedings*, 2124(1), pp. 1-14

Lin, Y-C., (1995), Maximum Specific Growth Rates of Mixed Anaerobic Populations as Psychrophilic Temperatures, *Master's Thesis*, United States.

Logan, B.E., (2008), *Microbial Fuel Cells*, John Wiley and Sons, Inc., New Jersey, pp. 451-456.

Mshandete, A., Björnsson, L., Kivaisi, A. K., Rubindamayugi, S. T., Mattiasson, B., (2005), Enhancement of anaerobic batch digestion of sisal pulp waste by mesophilic aerobic pre-treatment, *Water Research*, 39(8), pp. 1569–1575

Marcus, K.A., Torres, C.I., Rittmann, B.E., (2007), Conduction-based Modelling of the Biofilm Anode of a Microbial Fuel Cell, *Biotechnology and Bioengineering*, 98(6), pp. 1171-1182

Mulder, C., Hendriks, A. J., (2014), Half-saturation constants in functional responses, *Global Ecology and Conservation*, 2(1), pp. 161–169

O'Keefe, D., Chynoweth, D., (2000), Influence of phase separation, leachate recycle and aeration on treatment of municipal solid waste in simulated landfill cells, *Bioresource Technology*, 72(1), pp. 55–66

Ortiz-Martínez, V. M, Salar-García, M. J., de los Ríos, A. P., Hernández-Fernández, F. J., Egea, J. A., Lozano, L. J, (2015), Developments in microbial fuel cell modeling, *Chemical Engineering Journal*, 271(1), pp. 50-60

Owens, J.D. and Legan, J.D., (1987), Determination of the Monod Substrate Saturation Constant for Microbial Growth, *FEMS Microbiology Letters*, 46(4), pp. 419-432

Rabaey, K., Lissens, G., Siciliano, S. D., Verstraete, W., (2003), A microbial fuel cell capable of converting glucose to electricity at high rate and efficiency, *Biotechnology Letters*, 25(18), pp. 1531–1535

Ringeisen, B. R., Ray, R., Little, B., (2007), A miniature microbial fuel cell operating with an aerobic anode chamber, *Journal of Power Sources*, 165(2), pp. 591-597

Sakthiselvan, P., Meenambiga, S.S., Madhumathi, R., (2019), Kinetic Studies on Cell Growth, *Vels Institute of Science Technology and Advanced Studies*, 2(1), pp. 1-8

Scott, K., (2015), *Microbial Electrochemical and Fuel Cells. Fundamentals and Applications*, 1st Ed, Woodhead Publishing, Cambridge, pp. 180-186.

Suryaga K. Z., (2017), Influence of Wastewater Type and Electrode Spacing for Microbial Fuel Cell Performance, *Master's Thesis*, Institut Teknologi Bandung, Indonesia.

Ullah, Z., Zeshan., (2019), Effect of Substrate Type and Concentration on the Performance of a Double Chamber Microbial Fuel Cell, *Water Science and Technology*, 81(7), pp. 1336-1344

Wang, X., Wang, G., and Hao, M. (2015). Modeling of the Bacillus subtilis bacterial biofilm growing on agar substrate. *Computational and Mathematical Methods in Medicine*, 1-10.

Wong, Y.-S., Teng, T. T., Ong, S.-A., Morad, N., and Rafatullah, M., (2014), Suspended growth kinetic analysis on biogas generation from newly isolated anaerobic bacterial communities for palm oil mill effluent at mesophilic temperature, *RSC Adv.*, 4(110), pp. 64659–64667

Zeng, Y., Choo, Y. F., Kim, B.-H., Wu, P., (2010), Modelling and simulation of two-chamber microbial fuel cell, *Journal of Power Sources*, 195(1), pp. 79–89